2024 5th International Conference on Computer, Big Data and Artificial Intelligence (ICCBD+AI) | 979-8-3315-3399-1/24/$31.00 ©2024 IEEE | DOI: 10.1109/ICCBD-AI65562.2024.00069

Overlapping Tensor Train Completion with TV Regularization for Image Reconstruction*

1st Lang Mo
Department of Statistics and Data Science
Southern University of Science and Technology
Shenzhen, China
12332894@mail.sustech.edu.cn

2nd Wenwu Gong
Department of Statistics and Data Science
Southern University of Science and Technology
Shenzhen, China
gongww@sustech.edu.cn

3rd Lili Yang*
Department of Statistics and Data Science
Southern University of Science and Technology
Shenzhen, China
yangll@sustech.edu.cn

***Abstract*—In this paper, we propose a novel tensor completion framework, Overlapping Tensor Train Completion with TV Regularization (OTTC-TV), which integrates the strengths of both Overlapping Ket Augmentation (OKA) and Total Variation (TV) regularization. This framework addresses two critical limitations of traditional tensor completion methods based on the Tensor Train (TT) decomposition: poor recovery performance in high missing rate scenarios and block artifacts that disrupt image continuity. By leveraging OKA, our proposal reduces block artifacts and improves inter-block smoothness, overcoming the non-smooth transitions between blocks. TV regularization further ensures smoothness across the reconstructed tensor by penalizing abrupt gradient changes. The proposed model demonstrates superior performance in completing high-missing-rate color images while also providing greater flexibility in handling varying input tensor dimensions. Extensive experiments validate the effectiveness and adaptability of OTTC-TV in color image reconstruction tasks.**

***Index Terms*—Low-rank tensor completion, High missing rate, Total variation, Overlapping**

I. INTRODUCTION

Tensors, as a multidimensional data structure, have been widely applied in image processing, video analysis, medical imaging, and other multi-modal data research fields [1], [2], [3]. They can efficiently represent complex multidimensional interactions and restore missing information in color image reconstruction through Low-Rank Tensor Completion (LRTC) techniques [4], [5], [6]. Therefore, tensors play a crucial role in many fields, such as color image reconstruction[4]

The LRTC problem can be formulated as:

$$\min_{\mathcal{M}} \operatorname{rank}(\mathcal{M}) \quad \text{s.t.} \quad P_\Omega(\mathcal{M}) = \mathcal{T}, \tag{1}$$

where $\mathcal{M} \in \mathbb{R}^{n_1 \times n_2 \times \cdots \times n_d}$ is the target tensor to be recovered, and $\mathcal{T}$ is the observed tensor with missing entries [7]. The operator $P_\Omega(\cdot)$ is a projection operator. However, directly minimizing the tensor rank is NP-hard[8], [9], motivating the use of convex relaxations, such as minimizing the nuclear norm of the tensor's matricization along different modes [5].

Traditional methods encounter further difficulties in capturing complex multi-way interactions. Tensor completion based on low-rank structures, such as CANDECOMP/PARAFAC (CP)[10] and Tucker[11], offers potential solutions. However, CP and Tucker decompositions are computationally expensive, particularly due to the difficulty of estimating the CP rank and the imbalance in Tucker decompositions, where unfolded matrices can vary greatly in size [7].

The limitations of CP and Tucker have led to the development of more efficient alternatives like Tensor Train (TT) decomposition[7]. While TT decomposition effectively addresses these computational challenges, there remain certain shortcomings, particularly in handling large-scale tensors with missing or sparse observations.

TT decomposition factorizes a tensor into smaller core tensors, reducing computational complexity while preserving global correlations across modes. The TT rank [12] of a tensor $\mathcal{M}$ is defined as:

$$\operatorname{rank}_{\mathrm{TT}}(\mathcal{M}) = (\operatorname{rank}(\mathcal{M}_{(1)}), \ldots, \operatorname{rank}(\mathcal{M}_{(d-1)})). \tag{2}$$

TT-based methods have achieved success in tasks like image reconstruction [13], [14], [6], but challenges remain under high sparsity. They often fail to preserve local smoothness, resulting in block artifacts that degrade image quality, especially in color datasets. Additionally, high missing rates lead to poor recovery of underlying structures, and most TT frameworks struggle to adapt to varying tensor dimensions, limiting their versatility.

979-8-3315-3399-1/24/$31.00 ©2024 IEEE
DOI 10.1109/ICCBD-AI65562.2024.00069

Recent studies show that attention mechanisms and latent variable models significantly improve image reconstruction. Xie et al. proposed a spatial attention-guided facial editing method to capture fine-grained features [15], and Takagi and Nishimoto demonstrated high-resolution reconstruction from brain activity using latent diffusion models [16]. These works suggest that new frameworks must integrate both global and local information to handle sparsity and missing data effectively.

To overcome the limitations of traditional tensor completion methods in high-missing-rate scenarios, we propose a framework integrating Overlapping Ket Augmentation (OKA) with Total Variation (TV) regularization. OKA improves local consistency by introducing overlapping blocks, reducing block artifacts and ensuring smooth transitions. TV regularization complements this by penalizing abrupt gradient changes, enhancing global smoothness and improving the reconstruction of sparse data. The synergy between OKA and TV boosts both accuracy and adaptability, offering a robust solution for tensor completion, particularly in high-dimensional, large-scale datasets.

The main contributions of this paper are summarized as follows:

- We introduce a novel tensor completion framework that integrates **Overlapping Ket Augmentation (OKA)**, **Total Variation (TV) regularization**, and **Tensor Train decomposition**. This integrated approach effectively reduces block artifacts and significantly improves local smoothness, enhancing image reconstruction performance.
- Our method demonstrates superior performance in scenarios with **extremely high missing rates**, where other methods typically fail. By utilizing overlapping block structures and efficient local information sharing, Our framework maintains stability and robustness where traditional approaches collapse.
- The framework is highly **adaptable to tensor sizes** and different application scenarios. Its flexibility and scalability make it an effective and general solution for color image reconstruction tasks.

II. Preliminaries

A. Tensor Basics

Tensors generalize matrices to higher dimensions, with an order N tensor being an element of a product of N vector spaces. For instance, vectors and matrices are tensors of order 1 and 2, respectively. We denote tensors by calligraphic letters like $\mathcal{M}$, where $\mathcal{M} \in \mathbb{R}^{I_1 \times I_2 \times \cdots \times I_N}$. Mode-$k$ matricization flattens a tensor $\mathcal{M}$ into a matrix along its k-th mode, aligning the mode-k fibers as matrix columns. It is represented as $\mathbf{M}_{(k)} \in \mathbb{R}^{I_k \times (I_1 \ldots I_{k-1} I_{k+1} \ldots I_N)}$.

B. Tensor Train

A Tensor Train (TT) decomposition is a specific type of low-rank tensor decomposition that represents a high-order tensor as a sequence (or train) of lower-order tensors, also known as TT-cores. For a tensor $\mathcal{M} \in \mathbb{R}^{I_1 \times I_2 \times \cdots \times I_N}$, the TT decomposition expresses $\mathcal{M}$ as:

$$\mathcal{M}(i_1, i_2, \ldots, i_N) = \mathbf{G}_1(i_1)\mathbf{G}_2(i_2) \ldots \mathbf{G}_N(i_N), \quad (3)$$

where each $\mathbf{G}_k(i_k) \in \mathbb{R}^{r_{k-1} \times r_k}$ is a TT-core and r_k are the TT-ranks satisfying $r_0 = r_N = 1$.

C. Overlapping Ket Augmentation (OKA)

OKA divides the input tensor into smaller overlapping blocks, where adjacent blocks share elements to maintain continuity and smoothness across regions.

Let the input tensor be $\mathcal{I} \in \mathbb{R}^{I_1 \times I_2 \times I_3}$. OKA constructs a higher-order tensor $\mathcal{T}$ as:

$$\mathcal{T}[I_1 \times I_2 \times I_3] = \sum_{i_p, \ldots, i_1 = 1}^{4} \sum_{j=1}^{I_1} c_{i_p \ldots i_1 j} e_{i_p} \otimes \cdots \otimes e_{i_1} \otimes \mathbf{u}_j, \quad (4)$$

where p depends on the tensor size and overlap, and e_{i_k} are orthonormal bases.

The number of overlapping elements $n_{\text{overlapping}}$ is computed based on the tensor slice dimensions. For odd rows or columns, $n_{\text{overlapping}} = 3$, and for even, $n_{\text{overlapping}} = 2$:

$$n_{\text{overlapping}} = \begin{cases} 3, & \text{if } r \text{ (or } c) \bmod 2 = 1, \\ 2, & \text{if } r \text{ (or } c) \bmod 2 = 0. \end{cases} \quad (5)$$

OKA enhances tensor completion by preserving local continuity, making it more powerful than traditional methods, especially in high-missing-rate scenarios.

III. Proposed Framework

The core of our proposed tensor completion framework integrates two major techniques: Overlapping Ket Augmentation (OKA) and Total Variation (TV) regularization, both of which work synergistically to address the shortcomings of traditional tensor completion methods in scenarios with high missing rates.

OKA introduces an overlapping block structure, reducing block artifacts common in non-overlapping methods. Traditional Ket Augmentation (KA) methods improve tensor order but often result in discontinuities between blocks, degrading image quality in high-missing-rate scenarios [6]. OKA mitigates this by sharing boundary information between adjacent blocks, ensuring smoother transitions and preserving continuity. Additionally, it offers flexibility for non-square or prime-sized tensors [17], making it suitable for various applications.

However, relying solely on OKA poses challenges when the missing rate becomes excessively high. In such cases, overlapping block structures may still fail to provide sufficient information, causing the model to fall into local optima and deteriorating completion quality [18]. While OKA improves local smoothness, it lacks a global mechanism to ensure continuity across the entire tensor.

To address this limitation, we incorporate TV regularization, which is highly effective in enforcing smoothness across the entire tensor by penalizing abrupt changes in data gradients [1]. This enhances the model's robustness, especially when dealing with sparse datasets. By suppressing local discontinuities and preventing noise amplification in regions with missing data, TV regularization complements OKA, which focuses on local continuity. Together, they ensure both local and global smoothness, significantly improving the overall quality and stability of the reconstruction process, even in extreme sparsity conditions.

A. Model

In our model, the input tensor $\mathbf{M}$ is processed using OKA, transforming it into a higher-order tensor $\mathcal{T}(\mathbf{M})$. The general formulation of this transformation is expressed as:

$$\mathcal{T}[I_1 \times I_2 \times I_3] = \sum_{i_p,\ldots,i_1=1}^{4} \sum_{j=1}^{I_1} c_{i_p \ldots i_1 j} e_{i_p} \otimes \cdots \otimes e_{i_1} \otimes \mathbf{u}_j, \tag{6}$$

where p is determined by the size of the input tensor and the number of overlapping elements, and e_{i_k} represents the orthonormal bases used in the augmentation process. The overlapping number, denoted by $n_{\text{overlapping}}$, is computed recursively based on the tensor's dimensions, ensuring that adjacent blocks share elements and maintain local continuity. This overlapping strategy reduces block artifacts and enhances the smoothness of the tensor $\mathcal{T}(\mathbf{M})$.

After this preprocessing with OKA, the objective function of the model can be written as:

$$\begin{aligned} f(\mathbf{X}, \mathbf{Y}, \mathcal{M}) = \min_{\mathcal{M}, \mathbf{X}, \mathbf{Y}} \sum_{k=1}^{j-1} \frac{\alpha_k}{2} \|\mathbf{X}_k \mathbf{Y}_k - \mathbf{T}_{[k]}(\mathbf{M}_{[k]})\|_F^2 \\ + \lambda \mathrm{TV}(\mathcal{T}(\mathbf{M})), \end{aligned} \tag{7}$$

where $\mathbf{X} = (\mathbf{X}_1, \ldots, \mathbf{X}_{j-1})$, $\mathbf{Y} = (\mathbf{Y}_1, \ldots, \mathbf{Y}_{j-1})$, and λ is the regularization parameter. The first term is the fidelity term, while the second is the regularization term. The TV term promotes spatial smoothness in the tensor reconstruction.

B. Algorithm

We adopt a Block Successive Upper-Bound Minimization (BSUM) approach based on [19] to solve the non-convex tensor completion problem. The algorithm alternates between updating the matrices $\mathbf{X}_k$ and $\mathbf{Y}_k$ derived from the OKA-processed tensor and solving the $\mathcal{T}$-subproblem using ADMM, incorporating the TV regularization term.

1) BSUM: In each iteration of the BSUM framework, the following steps are performed:

The matrix $\mathbf{X}_k$ is updated by solving the following subproblem for each mode-k unfolding of the tensor:

$$\mathbf{X}_k^{l+1} = \left(\alpha_k \mathbf{T}_{[k]}^l (\mathbf{Y}_k^l)^\top + \rho \mathbf{X}_k^l\right) \left(\alpha_k \mathbf{Y}_k^l (\mathbf{Y}_k^l)^\top + \rho \mathbf{I}\right)^{-1}, \tag{8}$$

where ρ is a proximal parameter, $\mathbf{T}_{[k]}$ represents the mode-k unfolding of the current tensor $\mathcal{T}$, and α_k is a mode-specific weight.

After updating $\mathbf{X}_k$, the matrix $\mathbf{Y}_k$ is updated for each mode-k as follows:

$$\mathbf{Y}_k^{l+1} = \left(\alpha_k (\mathbf{X}_k^{l+1})^\top \mathbf{X}_k^{l+1} + \rho \mathbf{I}\right)^{-1} \left(\alpha_k (\mathbf{X}_k^{l+1})^\top \mathbf{T}_{[k]}^l + \rho \mathbf{Y}_k^l\right). \tag{9}$$

These alternating updates progressively refine the low-rank representation of the tensor at each iteration.

2) ADMM for $\mathcal{M}$ Subproblem: Once the matrices $\mathbf{X}_k$ and $\mathbf{Y}_k$ are updated, we solve for the tensor $\mathcal{T}$ by using the Alternating Direction Method of Multipliers (ADMM). The optimization problem to solve is:

$$\begin{aligned} \mathcal{T}^{l+1,p+1} = \arg\min_{\mathcal{T}} \sum_{k=1}^{j-1} \frac{\alpha_k}{2} \|\mathbf{X}_k^{l+1} \mathbf{Y}_k^{l+1} - \mathbf{T}_{[k]}\|_F^2 \\ + \frac{\rho}{2} \|\mathcal{T} - \mathcal{T}^l\|_F^2 + \lambda \mathrm{TV}(\mathcal{T}), \end{aligned} \tag{10}$$

where the TV regularization term promotes smoothness across tensor slices, and λ is the regularization parameter.

$$\mathcal{T}^{l+1} = \arg\min_{\mathcal{T}} \sum_{k=1}^{j-1} \|\mathbf{X}_k^{l+1} \mathbf{Y}_k^{l+1} - \mathbf{T}_{[k]}\|_F^2 + \lambda \mathrm{TV}(\mathcal{T}), \tag{11}$$

which updates the primary tensor variable by minimizing the fidelity term and TV regularization.

$$\mathbf{A}_k^{l+1} = \frac{\alpha_k \text{unreshape}(\mathbf{X}_k^{l+1} \mathbf{Y}_k^{l+1}) + \beta_1 \mathcal{M}^{l+1} + \mathbf{B}_k^{l+1}}{\alpha_k + \beta_1}, \tag{12}$$

which balances between the low-rank term and the updated tensor.

$$\mathbf{Z}^{l+1} = \arg\min_{\mathbf{Z}} \left(\|\mathcal{M}^{l+1} - \mathbf{Z} + \mathbf{Q}^{l+1}\|_F^2 + \beta_2 \|\mathbf{Z}\|_F^2\right), \tag{13}$$

enforcing the constraints involving $\mathbf{Z}$ and the TV regularization.

$$\mathbf{E}_k^{l+1} = \arg\min_{\mathbf{E}_k} \|\mathcal{T} - \mathbf{A}_k^{l+1}\|_F^2 + \lambda \mathrm{TV}(\mathbf{E}_k), \tag{14}$$

which ensures local smoothness and minimizes block artifacts.

After updating all auxiliary variables, the tensor $\mathcal{T}$ is projected back to the feasible set to satisfy the observed data constraints:

$$\mathcal{T}^{l+1} = \mathcal{P}_\Omega \left(\sum_{k=1}^{j-1} \mathbf{X}_k^{l+1} \mathbf{Y}_k^{l+1} + \mathcal{T}^{l+1}\right), \tag{15}$$

where $\mathcal{P}_\Omega(\cdot)$ is the projection operator that retains the observed entries and reconstructs the missing entries.

This iterative process guarantees that the tensor is completed with smooth transitions and robust performance, even for high missing rate scenarios.

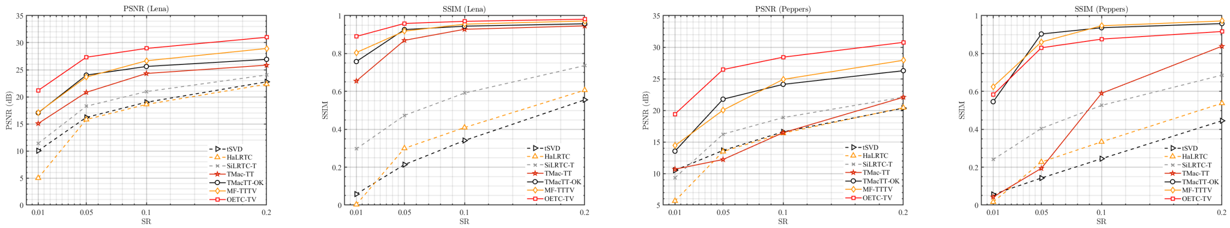

(a) PSNR (Lena) (b) SSIM (Lena) (c) PSNR (Peppers) (d) SSIM (Peppers)

Fig. 1: The PSNR and SSIM values for Lena and Peppers images.

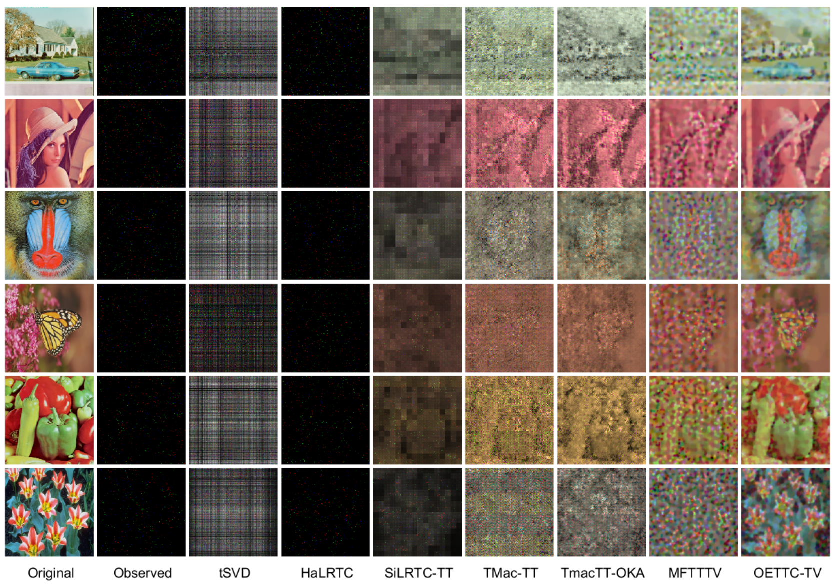

Fig. 2: Fig presents the visual comparison of color image reconstruction with a sampling rate (SR) of 0.01 using different tensor completion methods. The figure showcases the original image, followed by the observed (incomplete) data, and then the results obtained by several methods, including SiLRTC, TMac, TNN, SiLRTC-TT, TMac-TT, and MF-TTTV

IV. Numerical Experiments

A comprehensive evaluation of our model: Overlapping-enhanced Tensor Train Completion with TV regularization (OTTC-TV) will be presented in this section for color image reconstruction. The performance of OTTC-TV is compared against several state-of-the-art tensor completion techniques, including tSVD [20], HaLRTC [21], SiLRTC-TT [6], TMac-TT [6], TmacTT-OKA [18] and MFTTTV [19].

A. Experiment setting

Experiments are conducted across a diverse set of color image datasets, including *house*, *lena*, *mandril*, *monarch*, *peppers*, and *tulips*. The experiments are performed on resized images of dimensions $256 \times 256 \times 3$. For each dataset, the tensor completion methods are applied under sampling rates of 0.01, 0.05, 0.1, and 0.2, we use two widely recognized image quality metrics: Peak Signal-to-Noise Ratio (PSNR) and Structural Similarity Index (SSIM) to assess our model.

For each method, hyperparameters such as the regularization parameters λ and penalty parameters β are empirically optimized. The parameter λ was selected from the set $\{0.01, 0.03, 0.05, 0.1\}$ and β from $\{0.01, 0.03, 0.05, 0.1, 0.3\}$, with the aim of maximizing PSNR for each dataset.

B. Results and Analysis

Table I shows part of the results, providing PSNR and SSIM values for each method under different sampling rates. The results shows the superiority of our method, OTTC-TV, especially in scenarios with high missing rates. As the sampling rate decreases, most methods exhibit a significant decline in performance, struggling to maintain high-quality reconstructions. However, OTTC-TV consistently achieves the best performance across all sampling rates, particularly when

TABLE I: The PSNR and SSIM values

Image	SR	0.01		0.05		0.1		0.2	
	Method	PSNR	SSIM	PSNR	SSIM	PSNR	SSIM	PSNR	SSIM
house	tSVD	8.7628	0.0558	16.6647	0.2851	19.0234	0.4172	22.0994	0.6055
	HaLRTC	3.2760	0.0017	15.8987	0.3035	18.2523	0.4427	21.5805	0.6226
	SiLRTC-TT	10.5820	0.1897	16.5917	0.3729	18.6432	0.4886	21.5482	0.6624
	TMac-TT	13.4362	0.1614	17.2618	0.5064	21.5472	0.7803	23.4039	0.8409
	TmacTTOKA	15.4703	0.2415	20.1363	0.6710	22.7579	0.8278	24.3599	0.8745
	MFTTTV	14.9628	0.3311	19.9360	0.7226	23.0919	**0.8510**	26.0531	**0.9163**
	OTTC-TV	**18.1800**	**0.5271**	**23.4500**	**0.7482**	**25.2600**	0.8157	**27.7600**	0.8840
lena	tSVD	10.0404	0.0581	16.2044	0.2136	19.0021	0.3409	22.7725	0.5555
	HaLRTC	4.9989	0.0029	15.8031	0.2996	18.6024	0.4092	22.3349	0.6066
	SiLRTC-TT	11.4064	0.2966	18.2604	0.4732	20.9657	0.5913	24.0393	0.7362
	TMac-TT	15.0743	0.6549	20.8267	0.8696	24.3129	0.9280	25.8506	0.9458
	TmacTTOKA	17.0474	0.7576	24.0147	0.9263	25.6055	0.9442	26.9211	0.9571
	MFTTTV	17.1212	0.8050	23.6481	0.9182	26.6604	0.9551	28.9308	0.9718
	OTTC-TV	**21.1758**	**0.8902**	**27.3124**	**0.9587**	**28.9415**	**0.9700**	**30.9987**	**0.9810**

Algorithm 1 BSUM-based solver for OTTC-TV model

Input: Observed tensor $\mathcal{I} \in \mathbb{R}^{m\times n\times l}$, index set Ω, parameters α_k, ρ, λ, and maximum iterations $l_{\max}$, $p_{\max}$.
Output: Recovered tensor $\mathcal{T}$.
Preprocessing: Apply OKA to the input tensor $\mathcal{I}$ to obtain higher-order tensor $\mathcal{T}$.
Initialize $\mathbf{X}_0$, $\mathbf{Y}_0$, $\mathcal{T}_0$.
for $l = 1$ to $l_{\max}$ **do**
  for $k = 1$ to $j-1$ **do**
    Update $\mathbf{X}_k$ using:(8)
    Update $\mathbf{Y}_k$ using:(9)
  end for
  Update $\mathcal{T}$ using ADMM:
  $\mathcal{T}^{(l+1)} = \text{ADMM}(\mathbf{X}^{(l+1)}, \mathbf{Y}^{(l+1)}, \mathcal{T}^{(l)}, \Omega, \alpha_k, \rho, \lambda)$
  Check convergence criteria.
end for
Subroutine: ADMM_Sub($\mathbf{X}$, $\mathbf{Y}$, $\mathcal{T}$, Ω, α_k, ρ, λ)
Initialize auxiliary variables $\mathbf{A}_k$, $\mathbf{Z}$, $\mathbf{E}$, $\mathbf{B}_k$, $\mathbf{Q}$, $\mathbf{F}$.
for $p = 1$ to $p_{\max}$ **do**
  Update $\mathcal{T}^{(p+1)}$ using:(15)
  Update $\mathbf{A}_k$ using:(12)
  Update $\mathbf{Z}$ using:(13)
  Update $\mathbf{E}$ using:(14)
  Update $\mathbf{B}_k$, $\mathbf{Q}$, $\mathbf{F}$ using standard ADMM updates.
end for
return $\mathcal{T}^{(p+1)}$

the sampling rate drops to 0.01. The PSNR and SSIM values of OTTC-TV remain significantly higher than other methods, highlighting its robustness and effectiveness in handling highly sparse data. This suggests that the overlapping block structure and TV regularization work synergistically to preserve local smoothness and global structure, even in highly incomplete datasets.

Furthermore, the visual analysis in Figure 2 reveals that while most tensor completion methods collapse when the sampling rate is extremely low (e.g., 0.01), leading to distorted or unrecognizable images, OTTC-TV demonstrates remarkable resilience. It is capable of recovering recognizable and coherent images even in such extreme conditions. Other methods produce images that suffer from severe artifacts and blurred regions, making them difficult to interpret.

C. Ablation Study

Moreover, the ablation study further reinforces the effectiveness of both OKA and TV regularization in enhancing tensor completion performance. Specifically, the comparison between TMacTT, TMacTTOKA, MFTTTV, and OTTC-TV demonstrates the individual contributions of each component. TMacTT, which lacks any augmentation or regularization, consistently yields the lowest PSNR and SSIM values across all sampling rates, especially in high-missing-rate scenarios, indicating its limited ability to reconstruct sparse data. The introduction of OKA in TMacTTOKA leads to a noticeable improvement, reducing block artifacts by ensuring smoother transitions between overlapping regions. However, this enhancement alone is insufficient to address smoothness, particularly in more complex scenarios with higher missing data.

On the other hand, MFTTTV, which incorporates TV regularization, significantly improves global consistency by penalizing abrupt changes in data gradients, yielding higher PSNR and SSIM values than TMacTT and TMacTTOKA, especially as the sampling rate increases.

Ultimately, OTTC-TV, which combines both OKA and TV regularization, achieves the best results across all metrics. The synergistic effect of these two components not only reduces block artifacts but also maintains smoothness, making OTTC-TV an appropriate solution for tensor completion in highly sparse conditions. This underscores the necessity of both local and global enhancements to achieve superior reconstruction quality.

V. CONCLUSION

This paper proposes the Overlapping-enhanced Tensor Train Completion with TV regularization (OTTC-TV) for color image reconstruction under high-missing-rate scenarios. By integrating Overlapping Ket Augmentation (OKA) and Total Variation (TV) regularization, OTTC-TV mitigates block artifacts and enhances smoothness. Experiments show superior performance across various sampling rates.

Experimental results clearly demonstrate that OTTC-TV outperforms existing methods, both in numerical metrics and visual reconstruction quality. In high-missing-rate conditions (e.g., 95% missing),OTTC-TV retains key features and image structures while other methods fail to restore meaningful content.

Further research is needed to reduce the computational complexity introduced by TV regularization and OKA while maintaining performance.

ACKNOWLEDGMENT

This research is supported by the Educational Commission of Guangdong Province (Grant No. 2021ZDZX1069).

REFERENCES

[1] W.-F. Cao, Y. Wang, J. Sun, D.-Y. Meng, C. Yang, A. Cichocki, and Z.-B. Xu, "Total variation regularized tensor rpca for background subtraction from compressive measurements," *IEEE Transactions on Image Processing*, vol. 25, no. 9, pp. 4075–4090, 2016.

[2] M.-D. Iordache, J. M. Bioucas-Dias, and A. Plaza, "Total variation spatial regularization for sparse hyperspectral unmixing," *IEEE Transactions on Geoscience and Remote Sensing*, vol. 50, no. 11, pp. 4484–4502, 2012.

[3] T.-Y. Ji, T.-Z. Huang, X.-L. Zhao, T.-H. Ma, and L.-J. Deng, "A non-convex tensor rank approximation for tensor completion," *Applied Mathematics and Modeling*, vol. 48, pp. 410–422, 2017.

[4] J. Liu, P. Musialski, P. Wonka, and J. Ye, "Tensor completion for estimating missing values in visual data," *IEEE transactions on pattern analysis and machine intelligence*, vol. 35, no. 1, pp. 208–220, 2012.

[5] B. R. S. Gandy and I. Yamada, "Tensor completion and low-n-rank tensor recovery via convex optimization," *Inverse Problems*, vol. 27, no. 2, p. 025010, 2011.

[6] J. A. Bengua, H. N. Phien, H. D. Tuan, and M. N. Do, "Efficient tensor completion for color image and video recovery: Low-rank tensor train," *IEEE Transactions on Image Processing*, vol. 26, no. 5, pp. 2466–2479, 2017.

[7] I. V. Oseledets, "Tensor-train decomposition," *SIAM Journal on Scientific Computing*, vol. 33, no. 5, pp. 2295–2317, 2011.

[8] C. J. Hillar and L. H. Lim, "Most tensor problems are np-hard," *Journal of the ACM*, vol. 60, no. 6, p. 45, 2013.

[9] C. Mu, B. Huang, J. Wright, and D. Goldfarb, "Square deal: Lower bounds and improved relaxations for tensor recovery," in *International Conference on Machine Learning*, 2014, pp. 73–81.

[10] R. A. Harshman, "Foundations of the parafac procedure: Models and conditions for an explanatory multimodal factor analysis," 1970.

[11] L. R. Tucker, "Some mathematical notes on three-mode factor analysis," *Psychometrika*, vol. 31, no. 3, pp. 279–311, 1966.

[12] I. V. Oseledets, E. Tyrtyshnikov, and N. Zamarashkin, "Tensor-train ranks for matrices and their inverses," *Computational Methods in Applied Mathematics*, vol. 11, no. 3, pp. 394–403, 2011.

[13] L. Yuan, Q. Zhao, L. Gui, and J. Cao, "High-order tensor completion via gradient-based optimization under tensor train format," *Signal Processing: Image Communication*, vol. 73, pp. 53–61, 2019.

[14] C.-Y. Ko, K. Batselier, L. Daniel, W. Yu, and N. Wong, "Fast and accurate tensor completion with total variation regularized tensor trains," *IEEE Transactions on Image Processing*, vol. 29, pp. 6918–6931, 2020.

[15] M. Xie, S. Xiang, F. Wang *et al.*, "Spatial attention guided local facial attribute editing," in *Proceedings of the 2022 IEEE International Conference on Multimedia and Expo (ICME)*. IEEE, 2022, pp. 01–06.

[16] Y. Takagi and S. Nishimoto, "High-resolution image reconstruction with latent diffusion models from human brain activity," in *Proceedings of the IEEE/CVF Conference on Computer Vision and Pattern Recognition (CVPR)*. IEEE, 2023, pp. 14 453–14 463.

[17] J. I. Latorre, "Image compression and entanglement," *arXiv preprint quant-ph/0510031*, 2005.

[18] Y. Zhang, Y. Wang, Z. Han, Y. Tang *et al.*, "Effective tensor completion via element-wise weighted low-rank tensor train with overlapping ket augmentation," *IEEE Transactions on circuits and systems for video technology*, vol. 32, no. 11, pp. 7286–7300, 2022.

[19] M. Ding, T.-Z. Huang, T.-Y. Ji, X.-L. Zhao, and J.-H. Yang, "Low-rank tensor completion using matrix factorization based on tensor train rank and total variation," *Journal of Scientific Computing*, vol. 81, pp. 941–964, 2019.

[20] Z. Zhang and S. Aeron, "Exact tensor completion using t-svd," *IEEE Transactions on Signal Processing*, vol. 65, no. 6, pp. 1511–1526, 2016.

[21] J. Liu, P. Musialski, P. Wonka, and J. Ye, "Tensor completion for estimating missing values in visual data," *IEEE Transactions on Pattern Analysis and Machine Intelligence*, vol. 35, no. 1, pp. 208–220, 2013.